View metadata, citation and similar papers at core.ac.uk
brought to you by CORE
provided by Vietnam Academy of Science and Technology: Journals Online

Communications in Physics, Vol. 22, No. 1 (2012), pp. 65-73

PULSED ELECTRON DEPOSITION (PED) – A NOVEL TOOL FOR GROWTH OF THIN FILMS

NGO DINH SANG
National University of Civil Engineering
PHAM HONG QUANG AND DO QUANG NGOC
Hanoi University of Science, Vietnam National University

Abstract. *Pulsed Electron Deposition (PED) is a novel technique that can be applied for growing high quality thin films. In this technique, we used an electron beam with a focused diameter of about 1 mm, the energy up to 15 kV, the frequency of 1-10 Hz, the pulse width of 100 ns and the total current of 1.5 kA generated in a discharge system. A remarkable advantage of this technique is the low deviation in composition from bulk to film. By using the PED technique the transparent coducting ZnO and Cu(InGa)Se$_2$films were prepared. The effect of some deposition conditions on the properties of film has been examined and discussed. For Cu(InGa)Se$_2$, the best film was obtained at the discharge voltage of 12 kV and substrate temperature of 400°C, while for ZnO, the best film was grown at the oxygen pressure of 1.3 Pa and at 400°C.*

I. INTRODUCTION

Recently, Pulsed Electron Deposition (PED) has been attracting a great attention in thin film deposition [1-3]. This technique, also known as Channel-Spark Discharge and Pulsed Plasma Deposition, is based on a pulsed high power electron beam created in a low pressure gas discharge. The electron beams are characterized by short pulse widths (∼100 ns), high energy density (∼10 J/cm^2), and are delivered to a target surface by relatively low-energy electrons (∼10–20 keV), penetrating ∼1 mm into a target material, leading to a non-equilibrium heating that preserves the stoichiometric material transfer from the target to the substrate. PED shares some of the same advantages that characterize the well know technique, Pulsed Laser Deposition (PLD) such as easy control of film thickness, easy set-up, multicomponent film stoichiometry nearly identical to target material, and a relatively high deposition rate with low consumption of target materials. In addition, since electrons are charged particles, they interact very effectively via Coulomb interaction so that PED works for UV-transparent materials where PLD might fail. In fact, PED has been found to be useful for film deposition of complex materials such as superconductor, perovskite, oxides, and wide band gap semiconductor [4-6].

The structure of a CIGS based solar cell consists of several layers like the transparent conducting ZnO and the absorber Cu(InGa)Se$_2$ layers. Growth of pure ZnO films by PED has been reported by Porter *et al.* [7], Nistor et al. [8] , and Zhan *et al* [9]. And growth of CuInSe2 films by PED has been shown [10]. Andriesh *et al.* [11] also reported a two step deposition of $CuIn_{1-x}Ga_xSe_2$ polycrystalline films with a "e-beam ablation"

process followed by selenization at 500 ° C. In this work, we show a PED system that has recently been set-up at Hanoi University of Science and its ability in growth of transparent conducting ZnO and Cu(InGa)Se_2 films. Moreover, several issuers concerning the optimal growth conditions for getting good quality films have been shown.

II. PULSED ELECTRON DEPOSITION TECHNIQUE AND EXPERIMENTAL DETAILS

For the PED technique the channel spark system is used to produce a pulsed electron beam. The unit consists of a special type of hollow cathode, known as transient hollow cathode, a dielectric tube, which acts as an accelerator, and an air-filled spark-gap trigger tube for triggering the channel spark. For its operation the gas pressure in the system is maintained in the range of 0.7–2.7 Pa. By triggering the spark gap, constricted discharge is generated in the trigger tube, which ignites the transient hollow cathode. The electrons so generated form a beam and are accelerated through the dielectric tube. The general scheme of this process is shown in Fig. 1.

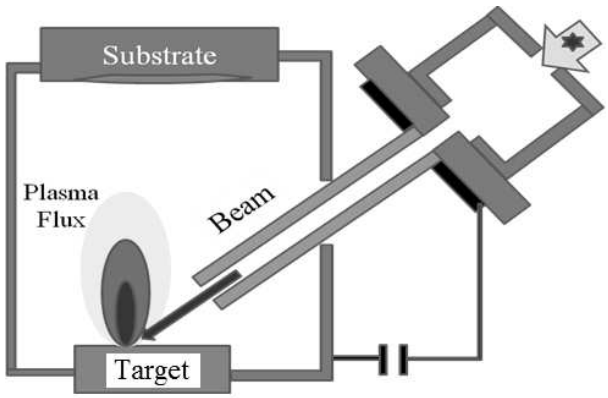

Fig. 1. General scheme of the PED process

In the beam, the mutual repulsion between the carriers is overcome by the magnetic self-field that keeps its trajectory self-focused and allows realization of the high current density of the beam [12]. The pulsed electron gun used in our experiments is a commercial source, PEBS-20 manufactured by Neocera, Inc. It has the following technical specifications: charging potential of 5-20 kV, beam energy of 0.2-0.8 J, pulse duration of 100 ns, maximum power density of 1.3×10^8W/cm^2, beam cross section of about 6×10^{-2}cm^2, repetition rate of 1-10 Hz. In order to enhances the uniform erosion and reduces the "conic effect" on the surface of target, a target rastering feature was made by the movement of the target stage at the X-Y plane about the central axis of the stage. Start angle, end angle, desired speed of rastering can be selected by the user using computer.

The CIGS films were deposited on glass substrate with the repetition rate of pulses maintained at 5 Hz and the argon pressure kept at 1 Pa, two series of CIGS films were prepared. The deposition of the CIGS-1 films was carried out at room temperature and

at four discharge voltages, viz., 8, 10, 12 and 14 kV. For the CIGS-2 films, the substrate temperature was ranged from room temperature to 600°C while the discharge voltage was kept at 12 kV. The target used in our work is a high purity commercial $Cu(In_{0.7}Ga_{0.3})Se_2$ which has a diameter of 2 inch and a thickness of 3 mm. All samples were deposited with 20,000 pulses.

Al-doped ZnO (AZO) thin films were deposited on quartz substrates. During growing process, the discharge voltage and the pulse frequency were maintained at 14 kV at 5 Hz, respectively. We chose the optimal potential discharge voltage of 14 kV as reported by Strikovski [13], with this voltage a maximal deposition rate can be obtained.. We also made two series of films; the series named AZO-1 was deposited at room temperature but at four pressures, viz., 0.7, 1.3, 2.0, 2.7 Pa of oxygen. The other series named AZO-2 was deposited at 1.0 Pa oxygen pressure but at the substrate temperatures ranged from 150°C to 600°C. During deposition process, the pressure was maintained by controlling the balance between the rate of high vacuum pump and the flow of oxygen gas introduced into the chamber. The target used is a high purity commercial 2 wt % Al_2O_3doped ZnO target having a diameter of 2 inch and a thickness of 3 mm. These samples were also deposited with 20,000 pulses.

The crystallinity of the films was checked by a Bruker-D5005 X-ray. Thickness of the films was determined by the stylus profiler (Detark-D150) and surface morphology was examined by SEM (Jeol-JSM5410LV). The optical properties were measured using UV-vis spectrophometer (UV-2450) in the wavelength range from 200 to 800 nm. The electrical resistivity was determined by four probe technique at room temperature.

III. RESULTS AND DISCUSSION

III.1. $Cu(InGa)Se_2$ films

The thickness of the CIGS-1 films was found to be 500, 650, 750 and 800 nm for the films grown at voltages of 8, 10, 12 and 14 kV, respectively. This result can be expected from the fact that the discharge voltage is the main factor determining the number of material ions created by ablation. For the CIGS-2 films, the thickness decreases slightly with increasing substrate temperature, corresponding to the enhancement of the crystallinity which will be mentioned below.

Fig. 2 shows the SEM images of some typical samples. For the CIGS-1 films, particulates in the range from 50 to about 100 nm are present on the surface of the films, whatever the value of discharge voltage. However, the density and the size of the particulates are smaller in the films deposited at lower voltage. The origin of these particulates is a matter of discussion. They can be directly emitted by the target during electron beam ablation, or they can be formed in the gas phase, during the transport of species from the target to the substrate. It is interesting to note that the surface morphology of the films was improved as increasing the substrate temperature. The film growth at 600°C has isolated grains with uniform size and well-defined boundaries, indicating a very good crystalinity. We have made an attempt to determine the composition of the films by using EDS but the result is not reliable due to the influence of the glass substrate.

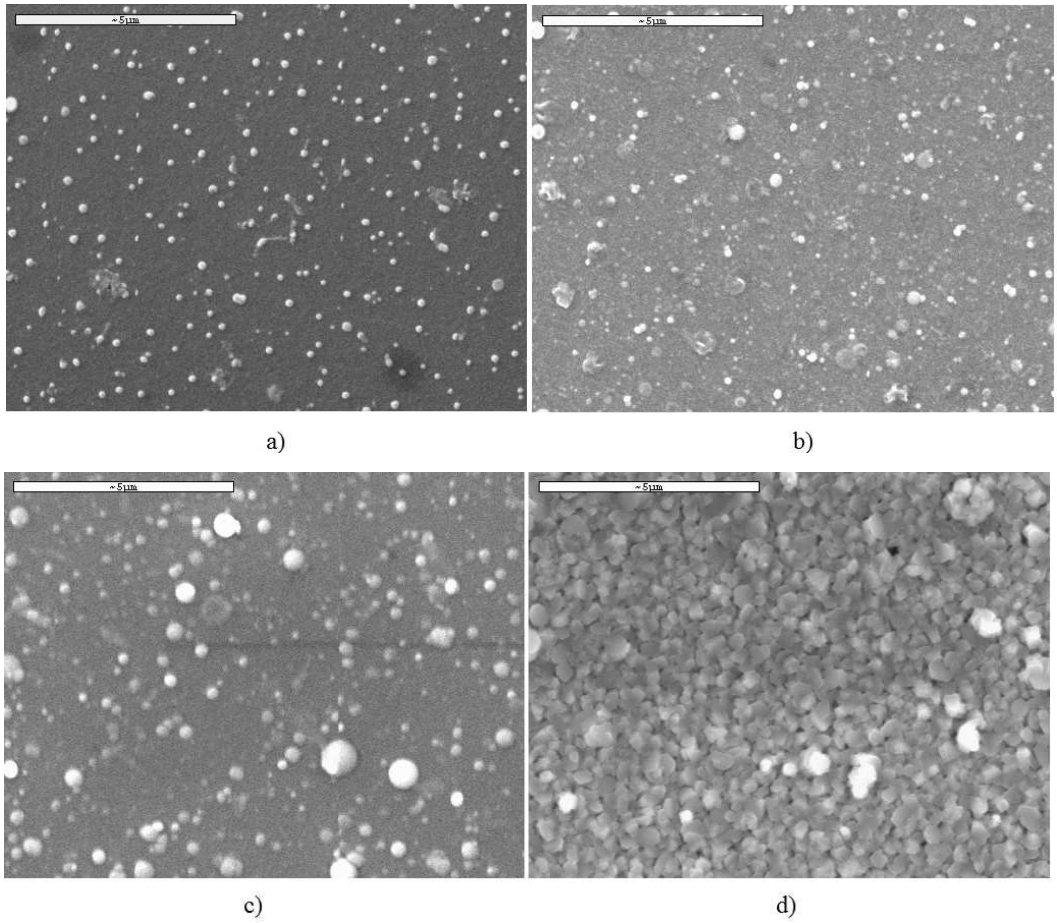

Fig. 2. (a),(b),(c) SEM images of CIGS-1 films grown at 8, 12 and 14 kV, respectively and (d) SEM image of CIGS-2 film grown at 12 kV and 600°C

The XRD patterns of CIGS-1 and CIGS-2 films are shown in Fig. 3(a) and 3(b), respectively. We can see that all CIGS-1 films (i.e. the films grown at room temperature) have an amorphous structure. The (112) peaks of chalcopyrite structure are observed in the XRD patterns of the CIGS-2 films, indicating the enhancement of crystalinity. These observations are in accordance with the SEM images. The orientation of the (112) peak and the grain size estimated by the full width at half-maximum of the (112) peak increase with increasing the substrate temperature. It is worth to note that the preference orientation of (112) face is a necessary requirement of the CIGS absorber layer for a high performance CIGS thin film solar cell. The improvement of the crystallinity is due to as the increase of the substrate temperature.

The absorption spectra of the CIGS-1 films have a tail in the transparent range which may be caused by the poor crystallinity of the films. Except the case of film growth at 150°C, the absorption spectra of the CIGS-2 films are typical for a direct

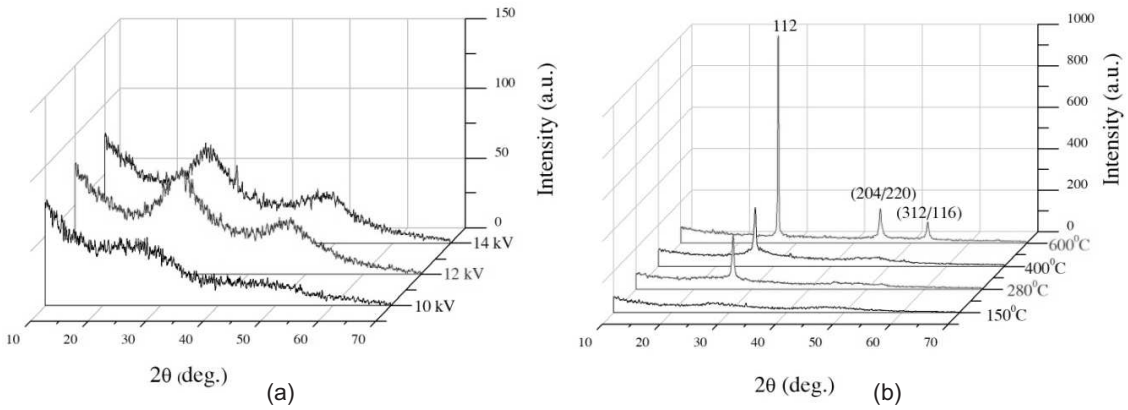

Fig. 3. The XRD patterns of (a) CIGS-1 films and (b) CIGS-2 films

band semiconductor which has a steep absorption edge. Fig. 4 shows the photon energy dependence of the square absorption coefficient for the films grown at 150°C, 280°C, 400 °C and 600°C. The band gap about 1.4 eV was determined by extrapolating the linear portion of these curves. This value of band gap is in agreement with the expected value for a bulk $Cu(In_{0.7}Ga_{0.3})Se_2$ sample [14]. It means that the stoichiometry of target materials is preserved in the film. It is very difficult to compare our results with those reported by Andriesh *et al.* [11] because their results were measured on the samples which have undergone the selenization process.

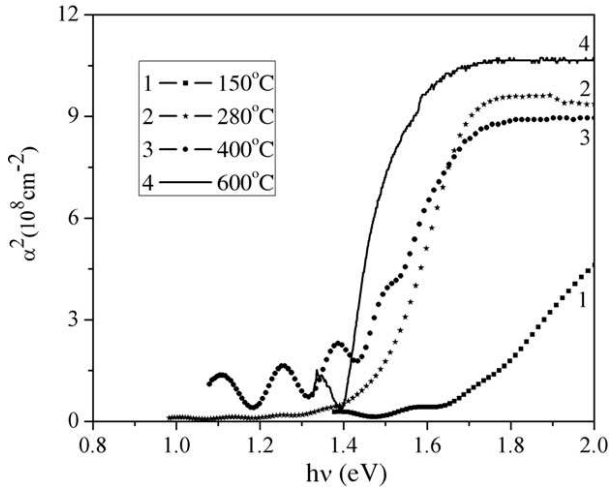

Fig. 4. The square of the absorption coefficient versus the photon energy curves for the CIGS-2 films

III.2. Al doped-ZnO

The thickness of the ZnO films is strongly dependent on the oxygen pressure. The thickness of the AZO-1 films is 270, 250, 230 and 220 nm for the films grown at 0.7, 1.3, 2.0 and 2.7 Pa oxygen pressure, respectively. The thickness of the AZO-2 films is almost identical with the value of about 250 nm. The decrease of the thickness with oxygen pressure can be can be attributed to the interaction between incoming ions in plasma flux and gas atoms, resulting in a decrease of current of ions arriving at the substrate. The SEM images of AZO (not shown) films are quite similar to those of CIGS films with the particals presenting on surface. Nistor *et al* also observed the similar problem [8] in growth of ZnO films and suggested the possibility to reduce it by careful optimization of the electron beam parameters in relation to the target materials.

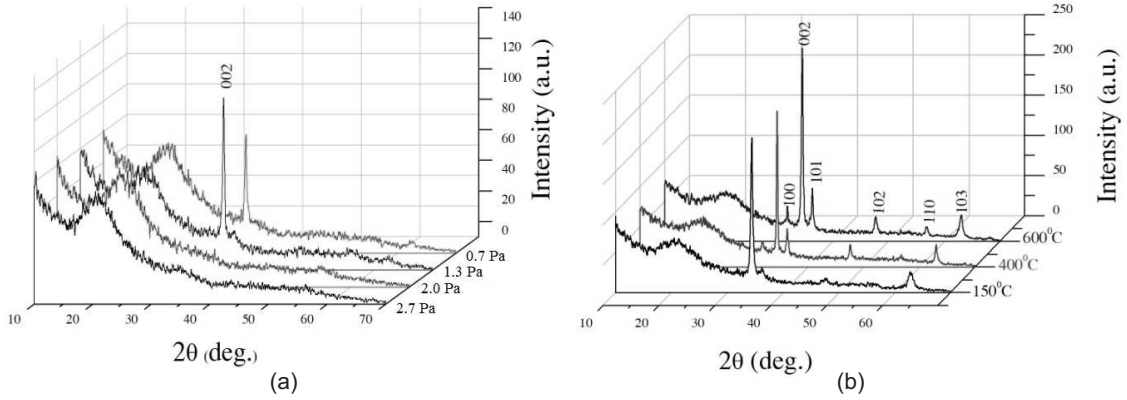

Fig. 5. The XRD patterns of the (a) AZO-1 films and (b) AZO-2 films

Fig. 5(a) shows the XRD patterns of the AZO-1 films. It is clear that the films grown at lower oxygen pressure (i.e. 0.7 and 1.3 Pa) exhibit a wurzite structure which has a highly preference for the (002) orientation whereas the films gown at higher oxygen pressure (i.e. 2.0 and 2.7 Pa) exhibit an amorphous structure. The highest intensity of (002) peaks for the film grown at 1.3 Pa indicates that this pressure is the most suitable. The degradation of the crystallinity at high oxygen pressure has also been observed by S. M. Park *et al.* in growth of AZO films by using PLD [15] and has been attributed to the excess oxygen that might induce defects in the films. P. Zhan *et al.* have also found that the oxygen pressure of 1.4 Pa is the most favorable value for obtaining the best crystallinity for the ZnO films grown by PED [9]. In our case, the effect of oxygen pressure seems to be stronger and more obvious because the films were grown at room temperature, so that the influence of temperature has been eliminated. The fact that oxygen pressure has an optimal value originates from the requirement of the average energy per deposited atom which should be about 10-20 eV. This energy in one hand is strong enough to complete the disruption of the columnar morphology of the growing film but in other hand do not damage the surface. It is well-known that in PED and PLD technique, with the presence

of background gases during ablation, the species arriving at substrate looses their average velocity as they undergo through scattering, thermalization and deceleration.

Fig. 5(b) shows the XRD patterns of the AZO-2 films. First of all, we can see that all films exhibit a wurzite structure with a highly preference for the c-axis orientation perpendicular to the substrate surface. The crystallinity evaluated from the intensity and full width at half-maximum of the (002) peak improves with increasing substrate temperature up to 400°C. Further increasing the substrate temperature leads to a slightly degradation in crystalinity. The grain size estimated from Scherrer equation is about 30 nm for the best film, i.e. the one deposited at 400°C. Hirata *et al.* [16], and Zhan *et al.* [9] have reported the similar effect of substrate temperature on the crystalinity of the ZnO films grown by PLD and PED. P. Zhan attributed the promotion of the (002) peak to the increase of adatom mobility as increasing substrate temperature. P. Zhan also explained the degradation of (002) peak at high temperature by structure zone model proposed by Thormton [17]. According to this model, the films deposited at high temperature (> 320°C for his case) have zone three structures which contain much more randomly oriented grains formed by secondary nucleation and recrystallization.

The electrical resistivity measured on the AZO-1 films is very high. However, it is still possible to realize that the resistivity is lower for the films deposited at lower oxygen pressure. The substrate temperature dependence of electrical resistivity of the AZO-2 films was presented in Table 1. As can be seen from this table, the resistivity decreases dramatically with increasing the substrate temperature up to 400°C, and then increases slightly again. Park *et al.* [9] have observed a similar phenomenon on undoped ZnO films grown by PLD and attributed the decrease of resistivity to the increase of both carrier concentration and carrier mobility. The slight increase in resistivity of the films grown at high temperature was explained by the contamination of C from quartz substrate. Hirata *et al.* [16] reported that resistivity of Ga-doped ZnO films deposited by PLD decreases with increasing deposited temperature up to 300°C which is the highest investigated temperature. Since the facts that there is a close relation between the crystallinity and conductivity and that our films are ZnO doped with Al, we suggest that the enhancement of conductivity is mainly due to the increase of number of Al atoms really activated in matrix oxide to produce extra electrons in the band. The resistivity of $3.4 \times 10^{-5}\Omega\times$m obtained at the optimal temperature is still quite high for requirement of TCO films. An additional process for improving electrical resistivity is necessary and will be studied in next future.

Table 1. The substrate temperature dependence of electrical resistivity of the AZO-2 films

Substarte temperature	Electrical resistivity
25°C	$\sim \quad 10^{-2}\Omega\times$m
150°C	$5\times10^{-3}\Omega\times$m
400°C	$3.4\times10^{-5}\Omega\times$m
600°C	$8\times10^{-5}\Omega\times$m

The optical transmittance of the films in both AZO-1 and AZO-2 series are very high (more than 80%) in the range of 350-900 nm. It is worth to note that there is a relation

between the crystallinity and the transmittance, e.g. the highest value of transmittance (∼90%) has been obtained for the film which has the best crystallinity. This value meets the application requirement of transmittance exceeding 80%. The relation between the crystallinity and the optical property can be seen more clearly from the absorption spectra. The absorption spectra of AZO-1 and AZO-2 films are shown in Fig. 6(a) and 6(b), respectively. The absorption spectra of AZO-1 films have a tail in the transparent zone while the absorption spectra of all AZO-2 films have a sharp absorption edge. The value of band gap about 3.2 eV deduced from absorption spectra is somewhat lower than the value of 3.37 eV measured on pure and bulk ZnO materials [18].

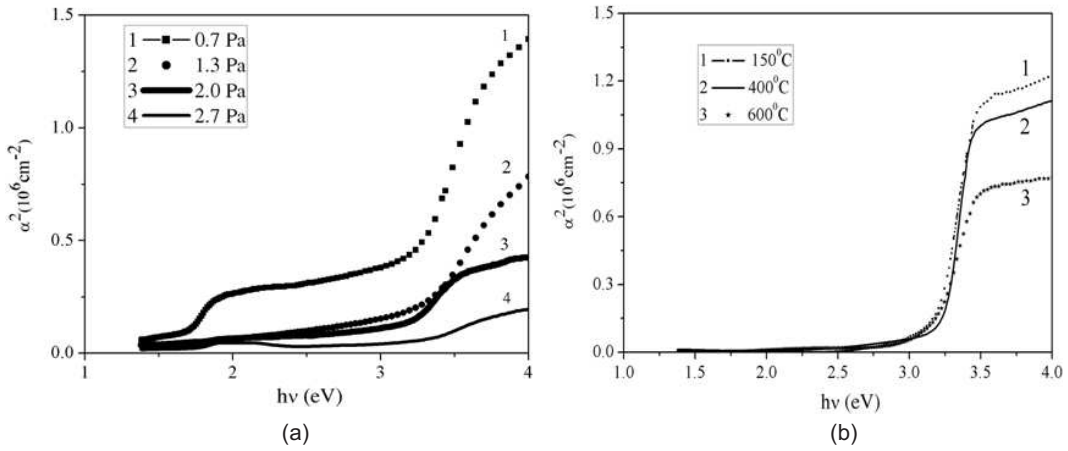

Fig. 6. The square of the absorption coefficient versus the photon energy curves for the (a) AZO-1 and (b) AZO-2 films

IV. CONCLUSION

By using a PED equipment that has been set-up at Hanoi University of Science the transparent conducting ZnO and Cu(InGa)Se_2 absorber films have been done. Several issuers concerning the optimal growth conditions for getting high quality films have been shown. For Cu(InGa)Se_2, the best film was obtained at the discharge voltage of 12 kV and substrate temperature of 400°C, while for ZnO, the best film was grown at the oxygen pressure of 1.3 Pa and at 400°C.

ACKNOWLEDGEMENTS

This work was supported by the Vietnam National Foundation for Science and Technology Development (NAFOSTED) in the period 2010-2011 (Project Code 103.02.59.09).

REFERENCES

[1] G. Muller, M. Konijnenberg, G. Krafft, and C. Schultheiss, in *Science and Technology of Thin Film*, edited by F. C. Matacotta and G. Ottaviani (World Scientific, Singapore, 1995), pp. 89–119.
[2] S. D. Kovaleski, R. M. Gilgenbach, L. K. Ang, and Y. Y. Lau, *J. Appl. Phys.* **86** (1999) 7129.

[3] R. Stark, J. Christiansen, K. Frank, F. Mücke, and M. Stetter, *IEEE Trans. Plasma Sci.* **23**, (1995) 258.
[4] X. L. Jiang and N. Xu, J. Appl. Phys. **66**, (1989) 5594.
[5] S. D. Kovaleski, R. M. Gilgenbach, L. K. Ang, and Y. Y. Lau, *Appl. Phys. Lett.* **73** (1998) 2576.
[6] R. Stark, J. Christiansen, K. Frank, F. Mucke, and M. Stetter, *IEEE Trans. Plasma Sci.* **23** (1995) 258.
[7] H. L. Porter, C. Mion, A. L. Cai, X. Zhang, J. F. Muth, *Material Science and Engineering* **B119** (2005) 210.
[8] M. Nistor, N. B Mandache and J. Perriere, *J. Phys. D: Appl. Phys.* **41** (2008) 165205.
[9] P. Zhan, Z. Li, and Z. Zhang, *Materials Transactions* **52**(9) (2011) 1764.
[10] G. Venkata Rao, G. Hema Chandra, P. Sreedhara Reddy, S. Uthanna, *J. Optoelectron. Adv. Mater.* **4** (2) (2002) 387.
[11] M. Andriesh, V. I. Verlan, L. A. Malahova, *Journal of Optoelectronics and Advanced Materials* **5**(4) (2003) 817.
[12] K. K. Jain and P. K. Sharma, *Appl. Phys. Lett.* **62** (1993) 1466.
[13] M. Strikovski and K.S. Harshavardhan, *Appl. Phys. Lett.* **82** (2003) 853.
[14] M. Marudachalam, R. W. Birkmire, H. Hichri, *J. Appl. Phys.* **82** (1997) 2896.
[15] S. M. Park, T. Ikegami, K. Ebihara, P. K. Shin, *Applied Surface Science* **253** (2006) 1522.
[16] G. A. Hirata, J. Mc Kitrick, J. Siqueiros, O. A. Lopez, T. Cheeks, O. Contreras and J. Y. Yi, *J. Vac. Sci. Technol.* **A14**(3) (1996) 791.
[17] J. A. Thornton, *Rev. Mater. Sci.* **7** (1977) 239.
[18] D. G. Thomas, *J. Phys. Chem. Solids* **15** (1960) 86.

Received 05 September 2011.